

Influence of Air Temperature on Dynamic Properties of Pipes Supplied with Pulsating Flow



Tomasz Pałczyński 

Abstract Air temperature has a significant influence on the dynamic properties of pipes supplied with pulsating flows. In many applications (power plants, pipelines, intake and exhaust systems for internal combustion engines), air temperature has an effect on resonance. Depending on the air temperature and its influence on transient flow parameters (pressure, temperature, density, speed of sound), there may be significant changes in the dynamic properties of the test pipe, such as resonant frequencies and the damping coefficient. In this study, experiments were conducted in an air temperature range of between 288 and 343 K, with a very a short air temperature step of around 5 K. Each measurement series was performed in triplicate. The results were processed in the Matlab environment using Fast Fourier Transforms. The empirical coefficients were visualized as 3D maps, including the influence of air temperature on pulsation dynamics in pipes. Finally, the experimental results were compared with the author's 1D model (based on the method of characteristics). The results are significant both for the theoretical understanding of flows in pipelines with pulsating flows and for practical applications in industry..

Keywords Air temperature · Pulsating flow · Dynamic properties

1 Introduction

Air temperature has a significant influence on the dynamic properties of pipes supplied with pulsating flows. In many applications (power plants, pipelines, intake and exhaust systems for internal combustion engines), air temperature has an effect on resonance. Depending on the air temperature and its influence on transient flow parameters (pressure, temperature, density, speed of sound), there may be significant changes in the pipe dynamic properties of the test pipe, such as resonant

T. Pałczyński (✉)

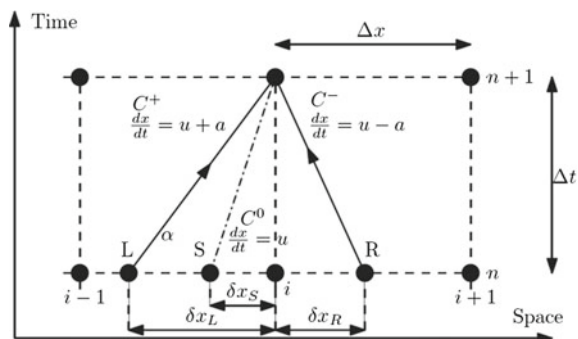
Flow Metrology Division, Institute of Turbomachinery, Lodz University of Technology,
219/223 Wólczańska Street, 90-924 Łódź, Poland
e-mail: tomasz.palczynski@p.lodz.pl

frequencies and the damping coefficient. Pulsating flow implies pulsating pressure, which causes vibrations and noise. It is thus one of the most important problems currently facing industry [1–3]. Numerous studies in the literature include mathematical modeling of the dynamics of pipeline systems interacting with a medium [4–9]. In this study, experiments were conducted into the amplitude and phase characteristics, resonant frequencies, damping coefficient and quality of approximation for pipes supplied with pulsating flows, fitted with relative nozzle diameters of between 3 and 9%. The experiments were supported by the author’s hybrid measurement method detailed in [10]. The National Instrument NI USB-6259 measurement card is designed to operate in the LabView environment, and is not supported by Matlab. Therefore, the experimental part of this project was based on LabView software. The second part, focusing on analog data processing, FFT (Fast Fourier Transform) analysis and Fourier series approximation, was conducted in Matlab. This clear division of process requirements demanded hybridization of the measurement process. Automated testing and recording was performed with LabView 2013 software. Calibration was performed using reference transmitters. Pressure transducers (Endevco 8510C-15 and 8510C-50) were calibrated using the glass tube water level gauge and a Vaisala PTB 330 reference barometer. Steady-state characteristics and performance were estimated using this procedure. Constant current thermometers (CCTs) were calibrated using a Type E reference thermoelectric element. Constant temperature anemometers (CTAs)—mass flow rate transducers—were calibrated using an Annubar-type flow meter. The experimental results were compared with the author’s 1D model, based on the method of characteristics (MOC).

2 Principles of Method of Characteristics

Benson’s [11] non-dimensional notation was used for first step approximation, where heat transfer and friction in pipes are often omitted (Fig. 1). The flow can be defined as homentropic, and there is no area section change. The two non-dimensional Riemann invariants (α and β) can be defined along the characteristics lines C^+ and C^- [12]:

Fig. 1 Method of characteristics in the space-time domain [12]



$$\alpha = A_i^{n+1} - \frac{\kappa - 1}{2} * U_i^{n+1} = A_R^n - \frac{\kappa - 1}{2} U_R^n, \quad (1)$$

$$\beta = A_i^{n+1} - \frac{\kappa - 1}{2} * U_i^{n+1} = A_L^n + \frac{\kappa - 1}{2} U_L^n, \quad (2)$$

where:

L, R, S nodes at time space domain due to C^+ , C^- , C^0 characteristics;

i space point;

n natural value in the time domain;

A non-dimensional speed of sound $A = \frac{a}{a_{ref}}$;

U non-dimensional velocity $U = \frac{u}{a_{ref}}$;

a_{ref} reference speed of sound

Using MOC, it appears that when all parameters at time step n are known, the Riemann characteristics (Eqs. 1 and 2) can be calculated. Using this information, the next step can be calculated.

For homentropic flow, contraction of the gas between S and the mesh node ($i, n+1$) can be defined:

$$\frac{p_S^n}{(\rho_S^n)^\kappa} = \frac{p_i^{n+1}}{(\rho_i^{n+1})^\kappa}, \quad (3)$$

Having found $\delta x_L, \delta x_R, \delta x_S$ (the distance between i node and L, S, R points) the thermodynamic states can be determined at nodes L, R and S using linear interpolation. There should be calculated: ρ_i^{n+1}, u_i^{n+1} , and p_i^{n+1} .

On the other hand, the transient speed of sound is determined as follows:

$$a = \sqrt{\kappa \cdot R \cdot T}, \quad (4)$$

where:

R individual gas constant 286,9 [J/(kg K)];

κ isentropic expansion factor;

T transient temperature (K);

a speed of sound (m/s)

Finally, the pipe length was estimated using the following equation:

$$f_n = \frac{a}{4 * L}, \quad (5)$$

where:

L pipe length (m)

Assuming the relationship presented above between the speed of sound, natural frequency and particle velocity, the following can be stated:

- (a) speed of sound strongly depends on the temperature of medium (Eq. 4);
- (b) the velocity of medium u is the additional speed propagating small amplitude disorders in air. This influences the course of the characteristic C^+ , C^- , C^0 lines, changing the dynamic properties of the analyzed pipes supplied with pulsating flows.
- (c) changes in the speed of sound change the natural frequency of the test pipe (Eq. 5).

3 Test Rig—Main Assumptions

The following assumptions were made:

- Real measurements taken of transitional states during pulsation frequency changes (from 20 to 180 Hz) in pipes. The main features of the test rig are presented in Fig. 2, including the pulse generator (PG) and three control sections (1, 2, 3).
- A simplified Simulink model, designed to estimate the local pulsation amplitude and amplitude-frequency characteristics [10].
- An analysis of the influence of frequency change in a range of amplitudes from 20 to 180 Hz on air pressure during pulsation changes at three control sections.
- Measurements showing resonant frequency changes with increasing and decreasing pulsation frequencies.
- Proposed parameters for estimating second-order inertial elements (the damping coefficient and resonant frequency), to describe the observed phenomena.
- Assessment of the impact of the sine swept constraint on amplitude-frequency characteristics.

The main parameters were as follows:

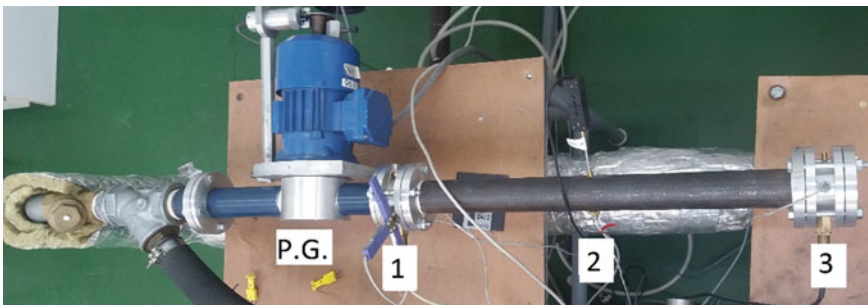


Fig. 2 Main elements of the test rig [1]. P.G.—pulse generator, 1, 2, 3—tested cross sections

- Range of desired values for the frequency of the pulse generator $f = (20 \div 180)$ (Hz).
- Pipe diameter $D_p = 42 \times 10^{-3}$ (m).
- Pipe length $L_p = 0.544$ (m), determined with resonance at 70 and 140 Hz.
- Nozzle diameters $D_n = 7.5 - 12.5 \times 10^{-3}$ (m). The nozzles were mounted at one end of the pipe, at cross section (3).
- Desired flow temperature from 313.15 to 343.15 (K).

Transient and mean values for pressure, temperature and specific mass flow rate were measured at control sections (1) and (3), shown in Fig. 2. Transient pressure was also measured in section (2), located in the middle of the length of pipe. Analysis of the dynamic properties of the pipe was performed using the second-order oscillating element as the reference, parametrizing objectively the differences between particular cases. It was thereby possible to approximate the swept frequency probe with a coefficient of determination greater than 95% ($R^2 > 0.95$). Second-order oscillating elements were estimated using Eq. (6) and the Curve Fitting Tool, with custom equation settings and default 95% confidence bounds [13]:

$$M(f) = \left\{ \left[1 - \left(\frac{f}{f_n} \right)^2 \right]^2 + \left[\frac{2\zeta f}{f_n} \right]^2 \right\}^{-1/2}, \tag{6}$$

where:

- $M(f)$ magnitude of oscillations (-)
- f_n natural frequency (Hz)
- ζ relative damping coefficient (-)

Resonant frequency was calculated using the equation [13]:

$$f_r = f_n \sqrt{1 - \zeta^2}, \tag{7}$$

Magnitude of oscillations were calculated as an relative amplitude of oscillations from the cross section 2 or 3 referenced to cross section 1.

4 Experimental and Simulation Results

Table 1 shows values for the damping coefficient and resonant frequencies in the studied cases. Each three rows represent the same temperature for three investigated mass flows (20, 24, 28 kg/s). The first group of columns represents experimental results according to p_3/p_1 (quotient of pressure pulsation of the third to the first cross-section) and the second group p_2/p_1 (quotient of pressure pulsation of the second to the first cross section). For each group, the natural frequency and relative damping coefficient were estimated (Eq. 1), together with R^2 —the coefficient of

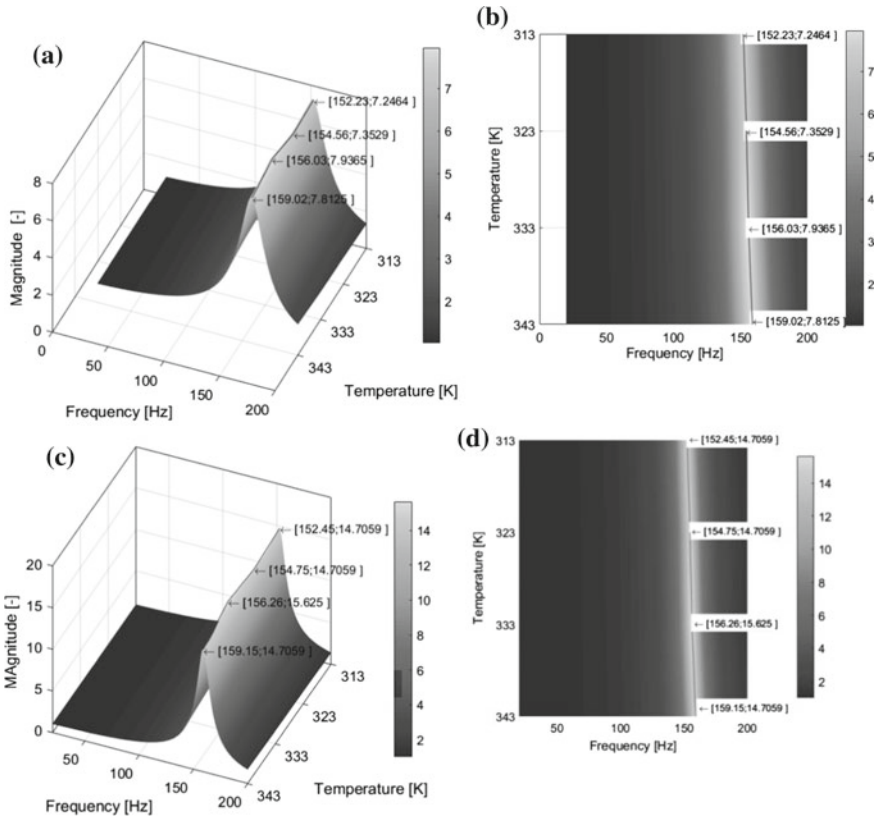


Fig. 3 **a** Magnitude p_2/p_1 —3D plot in the frequency and temperature domains. **b** Magnitude p_2/p_1 —contour plot in the frequency and temperature domains. **c** Magnitude p_3/p_1 —3D plot in the frequency and temperature domains. **d** Magnitude p_3/p_1 —contour plot in the frequency and temperature domains

determination and resonant frequency (Eq. 2). The whole spectrum of investigated temperatures was from 313.15 to 343.15 K with a 10 K step.

Figure 3 presents magnitude–frequency characteristics in the temperature domain. Figure 3a shows magnitude for p_2/p_1 as a 3D map in the frequency and temperature domains. Figure 3b provides a view from above, to show more clearly the influence of air temperature. As can be seen, air temperature increases from 313.15 to 343.15 K as resonant frequency increases from 152 to 159 Hz (4.5%). Similarly, Fig. 3a shows magnitude for p_3/p_1 as a 3D map in the frequency and temperature domains. A view from the top is presented in Fig. 3d to make more visible the influence of air temperature. As can be seen, air temperature increased from 313.15 to 343.15 K as resonant frequency increased from 152 to 159 Hz (4.5%).

In Fig. 4, there is significant noticeable increase from 7 to 14 magnitudes due to movement from the second to the third cross section.

Table 1 Experimental results

Temp. (K)	Mass flow (kg/s)	p_3/p_1				p_2/p_1			
		f_n (Hz)	Z (-)	f_r (Hz)	R^2 (-)	f_n (Hz)	ζ (-)	f_r (Hz)	R^2 (-)
313,15	20	152.44	0.043	152.16	0.850	151.78	0.083	151.72	0.984
313,15	24	152.45	0.034	152.16	0.860	152.23	0.069	151.51	0.973
313,15	28	152.64	0.029	152.51	0.870	151.51	0.053	151.08	0.986
323,15	20	154.81	0.043	154.52	0.870	154.53	0.084	153.44	0.990
323,15	24	155.81	0.032	155.52	0.850	156.42	0.061	153.50	0.863
323,15	28	154.76	0.028	154.64	0.878	154.37	0.055	153.91	0.997
333,15	20	157.17	0.041	156.91	0.882	156.83	0.079	155.83	0.994
333,15	24	156.26	0.032	156.10	0.876	156.03	0.063	155.41	0.996
333,15	28	156.92	0.025	156.82	0.894	156.85	0.050	156.45	0.988
343,15	20	158.72	0.040	158.46	0.895	158.85	0.079	157.86	0.987
343,15	24	158.66	0.030	158.52	0.898	158.25	0.057	157.73	0.973
343,15	28	157.95	0.025	157.18	0.829	158.59	0.055	157.73	0.972

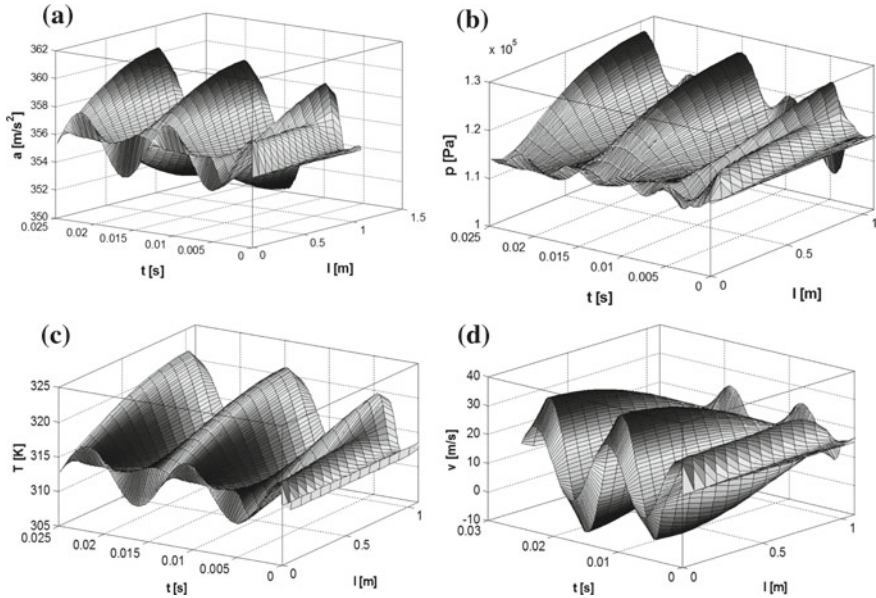


Fig. 4 Numerical simulation results for the resonant frequency $f_r = 145.16$ (Hz) and nozzle diameter 10×10^{-3} m and temperature 313,15 K: **a** local speed of sound in the time-space domain, **b** transient pressure in the time-space domain, **c** transient temperature in the time-space domain, **d** particle transient velocity in the time-space domain

The amplitudes of the oscillations at cross sections 1 and 2 were estimated and the magnitudes p_2/p_1 calculated. Magnitudes were assigned to the pulse generator frequencies. The coefficient of determination for the magnitude curve approximation is very good for p_2/p_1 , with an average value $R^2 = 0.98$ and for p_3/p_1 the average value is $R^2 = 0.87$. This proves that the second-order oscillating element is sufficient for approximating the dynamic states of pulsating flows in pipes with partially-closed ends, including the influence of air temperature and the mass flow rate (especially for p_2/p_1 cases).

Calculations using the Simulink model (based on the method of characteristics) were performed in parallel with the experimental studies. Sample simulation results are presented in Fig. 4, which shows flow parameters in the time-space domain. The simulation of acoustic phenomena for the initial time steps is clearly visible. The propagating wave is divided into two parts, and is proportional to the cross-section area change coefficient. The reflected part of the propagating wave has closed-end type boundary conditions. The rest of the falling wave propagates outside the nozzle. Qualitative comparison of the results of the numerical studies reveals a good match with experimental measurements.

The assumed air temperature change was confirmed. The assumed reference speed of sound conditions for the partially-closed end were verified against the model of air temperature. Acoustic phenomena were confirmed for the analyzed flows. Nodes

and antinodes were found for the standing wave. At resonant frequency pulsations, the pressure nodes were located at the beginning of the pipe. Velocity antinodes can also be seen at the pipe end (cross section 3).

4.1 Experimental and Simulation Results—Discussion

Figures 5 and 6 provide a graphical interpretation of the results from Table 1. The influence of the mass flow rate and air temperature on the relative damping coefficient was estimated for p_3/p_1 (quotient of pressure pulsation of the third to the first cross-section) and p_2/p_1 (quotient of pressure pulsation of the second to the first cross-section).

A significant decrease in the relative damping coefficient can be noticed, due to the increase in the mass flow rate. Case p_3/p_1 has much lower values for the relative damping coefficient, compared to p_2/p_1 . This is caused by the flow phenomenon illustrated in Fig. 4b. The amplitudes of the pressure pulsation in the middle length of the tested pipe are lower. In the case of p_2/p_1 , with a low mass flow rate there is a slight decrease in the relative damping coefficient, from 0.083 to 0.079 (−5%). A significant decrease in the relative damping coefficient was observed, from 0.069 to 0.057 (−21%), in the case of p_2/p_1 with medium mass flow rates [24 (kg/s)]. In the

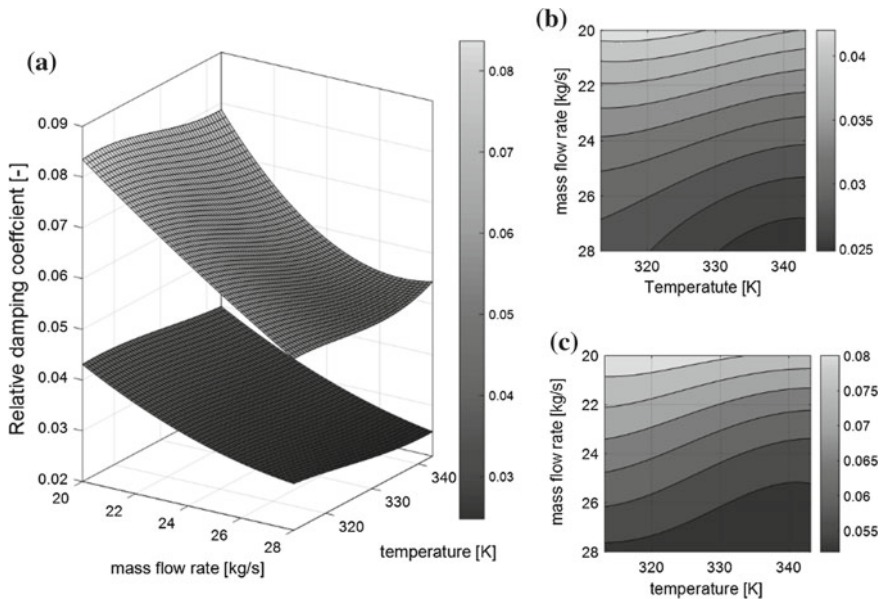


Fig. 5 a Damping coefficient relative to mass flow rate and air temperature (p_3/p_1 upper, p_2/p_1 bottom). b 2D plot—damping coefficient relative to mass flow rate and air temperature p_2/p_1 . c 2D plot—damping coefficient relative to mass flow rate and air temperature p_3/p_1

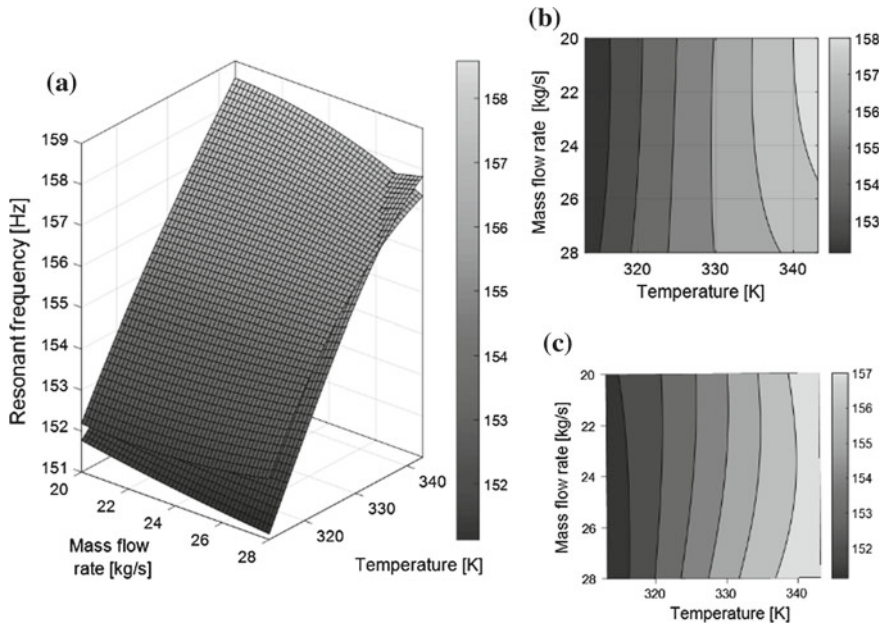


Fig. 6 a Resonant frequency relative to mass flow rate and air temperature (p_3/p_1 upper, p_2/p_1 bottom). b 2D plot—resonant frequency relative to mass flow rate and air temperature p_2/p_1 . c 2D plot—resonant frequency relative to mass flow rate and air temperature p_3/p_1

case of p_3/p_1 , the influence of air temperature on the relative damping coefficient was very slight. However, the mass flow rate was found to have a significant influence on the relative damping coefficient in both cases p_3/p_1 and p_2/p_1 . In the case of p_3/p_1 , there is a significant decrease in the relative damping coefficient, from 0.043 to 0.029 (−48%) at low temperatures, independent of air temperature. The decrease in the relative damping coefficient in case p_3/p_1 is greater at high air temperatures, from 0.040 to 0.025 (−60%). In the case of p_2/p_1 , there is a significant decrease in the relative damping coefficient, from 0.083 to 0.053 (−57%).

The impact of air temperature and mass flow rate on resonant frequencies stands in contrast to the variability of the relative damping coefficient. Of course, this contrast is only apparent because these physical quantities were conjugated in the manner presented above. Changes in resonant frequencies with changes in air temperature were also significant, with an increase of around 9% (from 313.15 to 343.15 K), increasing to 3.2% (from 152.16 to 157.18 Hz) in the case of p_3/p_1 and increasing to 3.8% (from 151.72 to 157.73 Hz) in the case of p_2/p_1 .

The significant influence of air temperature on the relative damping coefficient, and of mass flow rate on resonant frequencies, is of great importance for understanding the dynamic properties of pipes supplied with pulsating flows. All kinds of pipelines and compressed air lines suffer due to vibrations induced by resonance frequencies. The experimental results presented in Figs. 5 and 6 as three-dimensional

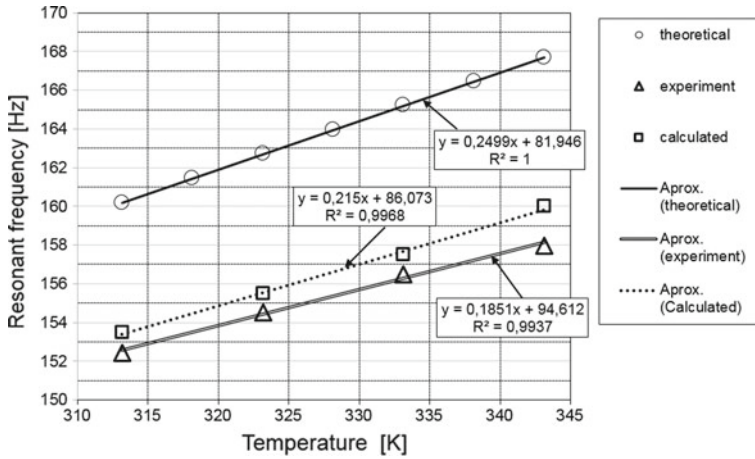


Fig. 7 Resonant frequency versus temperature (theoretical, experimental and calculated from simulation model based on MOC)

maps of the real relative damping coefficient and resonant frequencies could be used as corrective steering or process engineering maps. The research results presented here could also help to protect large industrial systems against defects caused by uncontrolled changes in the dynamic characteristics of pipelines.

A comparison of the theoretical (Eq. 5) and experimental results is presented in Fig. 7. The much higher theoretical resonant frequencies are caused by the simplicity of Eq. 5, which does not take into account the cross-section area change coefficient (due to the use of a nozzle 10×10^{-3} m in diameter at the end of pipe). The directional factor of the empirical resonant frequency characteristics is lower in comparison with the theoretical value (by around 25%). The calculated resonant frequencies are similar to those measured experimentally. Generally, the experimental results are comparable with those of the numerical studies. The differences identified were caused by the simplicity of the 1D model used, based on MOC.

The resonance phenomenon is very often used in internal combustion engines as a dynamic boost intake system (significantly improving filling efficiency) and in the exhaust system (significantly lowering exhaust losses). The research presented here has very important implications for the automotive industry, due to significant influence that the dynamic properties of manifolds with pulsating flows have on the efficiency and environmental performance of internal combustion engines. The resonance phenomenon was also observed closely in automobile intake and exhaust manifolds. Intake and exhaust systems generally operate with various mass flow rates and at different temperatures. During the research, there were audible signs which confirmed the observed resonance phenomenon. The author is planning a synthesis of the measurement methods used in the presented studies with acoustic research, to objectify the acoustic impressions from pipes tested with pulsating flows.

5 Conclusions

Air temperature and mass flow rate have a significant influence on the dynamic properties of pipes supplied with pulsating flows. This paper has presented the results of a quantitative and qualitative investigation into the influence of both the air temperature and the mass flow rate. Numerical modeling and experimental studies were performed in parallel and showed quite close agreement. Understanding changes in the dynamic properties of pipes supplied with pulsating flows is essential for the construction and operation of all kinds of pipelines and compressed air lines, which suffer due to vibrations induced by resonance frequencies. The results presented here are very important for the mathematical modeling, design and control of pipeline systems interacting with mediums such as compressed air in a wide range of pipeline systems, especially compressed air ducts, internal combustion engine inlets and exhaust systems.

Acknowledgements The author gratefully acknowledges the helpful comments and suggestions of the reviewers, which have improved the manuscript.

References

1. He, S., Jackson, J.: An experimental study of pulsating turbulent flow in a pipe. *Eur. J. Mech. B/Fluids* **28**, 309–320 (2009)
2. Park, J.-I., Adams, D., Ichikawa, Y., Bayyouk, J.: Frequency response of pressure pulsations and source identification in a suction manifold. *J. Sound Vib.* **277**, 669–690 (2004)
3. Dowling, J., Peat, K.: An algorithm for the efficient acoustic analysis of silencers of any general geometry. *Appl. Acoust.* **65**, 211–227 (2003)
4. Samuelson, R.D.: A second order system model for pneumatic instrumentation lines. *IEEE Trans. Nucl. Sci.* **16**(1), 271–276 (1969)
5. Howel, P.D., et al.: Mathematical analysis of the dynamic flow characteristic in a damping nozzle for a pressure transmitter. *J. Phys.: Conf. Ser.* **52**, 83 (2006)
6. Vetter, G., Seidl, B.: Pressure pulsation dampening methods for reciprocating pumps. In: *Proceedings of the 10th International Pump Users Symposium*, Houston, Texas, vol. 19 (1993)
7. Metwally, M.: Review of compressible pulsating flow effects on system performance. In: *13th International Conference on Aerospace Sciences & Aviation Technology, ASAT-13*, 26–28 May 2009
8. Cyklis, P., Młynarczyk, P.: The influence of the spatial discretization methods on the nozzle impulse flow simulation results. *Procedia Eng.* **157**, 396–403 (2016). ISSN 1877-7058. <https://doi.org/10.1016/j.proeng.2016.08.382>
9. Jungowski, W.: *Podstawy dynamiki gazów*, pp. 101–105. WPW, Warszawa (1972)
10. Pałczyński, T., Rydlewicz, W.: Hybrid method for researching pulsating flows in pipes exemplified with orifice application. In: *Advances in Condition Monitoring of Machinery in Non-Stationary Operations*, pp. 309–317. Springer, Cham (2018)
11. Benson, R.S.: One-dimensional transient flow in a pipe with two gases. *The Engineer* **202**, 687–691 (1956)
12. Pałczyński, T.: A hybrid method of estimating pulsating flow parameters in the space-time domain. *Mech. Syst. Signal Process.* **89**, 58–66 (2017)
13. Olczyk, A.: Identification of dynamic phenomena in pipes supplied with a pulsating flow of gas. *Proc. Inst. Mech. Eng. Part C: J. Mech. Eng. Sci.* **223**(8), 1851–1867 (2009)